

# Towards optimal fillet portioning: a computer vision system for determining the fish fillet volume

Chanh-Nghiem Nguyen<sup>1,2</sup>, Ngoc-Tan Vo<sup>1,2</sup>, Ngoc-Thanh Nguyen<sup>1,2</sup>, Nhut-Thanh Tran<sup>2</sup>,  
Chi-Ngon Nguyen<sup>2</sup>

<sup>1</sup>Automation Laboratory, Can Tho University, Can Tho, Vietnam

<sup>2</sup>Faculty of Automation Engineering, Can Tho University, Can Tho, Vietnam

## Article Info

### Article history:

Received Apr 11, 2024

Revised Aug 11, 2024

Accepted Aug 20, 2024

### Keywords:

Catfish

Computer vision

Fillet portioning

Laser light

Vision-based system

Volume measurement

## ABSTRACT

Portioning large fish fillets for packaging is usually performed manually by skilled workers. Automating this process and obtaining packaged products with attractive shapes and affordable weights will be beneficial for promoting purchase decisions. Towards developing an automated fish fillet portioning system, this study investigated a computer vision approach for determining the fillet volume. A belt conveyor would transport a fish fillet to the image capture booth, where its cross-section areas would be calculated for volume determination. The developed system could be operated with a conveyor speed ranging from 7.5 to 30.6 mm/s. The system performance was evaluated at a conveyor speed of 7.5 mm/s using small catfish fillets from 142.2 to 225.4 cm<sup>3</sup>. A mean percent error of 9.2% was observed, and the smallest percent error of 3.8% was obtained with a 225.4 cm<sup>3</sup> fillet. With minor measurement errors obtained for larger fillets, the proposed computer vision system showed great potential for developing a cost-effective automated system for customized fish fillet partitioning to accelerate purchase decisions and also for quality control and classification of the fish fillets.

This is an open access article under the [CC BY-SA](https://creativecommons.org/licenses/by-sa/4.0/) license.



## Corresponding Author:

Chanh-Nghiem Nguyen

Faculty of Automation Engineering, Can Tho University

Campus II, 3/2 Street, Ninh Kieu District, Can Tho City, Vietnam

Email: ncnghiem@ctu.edu.vn

## 1. INTRODUCTION

Fish are among the healthiest foods and are rich in essential nutrients, including high-quality proteins, various fatty acids, minerals, and vitamins [1]. Fish consumption was also linked to health benefits; for example, a reduction in coronary heart disease and stroke was reported with an increased fish intake [2], [3]. As a result, the consumption of fish or seafood in general has been a part of national dietary recommendations in many countries, particularly in most countries in Europe [4]. However, the daily or weekly recommended serving differed in many national guidelines, which could be a fixed amount or within a recommended range [4], [5].

Fish products sold at local markets are available in different presentation formats, such as whole fish, fish steaks, fish fillets, round cuts, and ready-to-cook products. Among these formats, fillets are preferred over alternatives [6], [7], probably due to their ease of preparation [7], [8]. It was reported that consumers were generally willing to pay a premium price for fish fillets [7], [9]. Thus, large fish fillets should be sliced into smaller volumes that fall within the recommended serving ranges. This “good-for-health” information would encourage fish consumption because consumers would consent to paying higher premiums with health claims, as reported in [7].

A few studies have reported good relationships between a few morphometric parameters and fish weight. For example, the coefficient of determination reached 0.9822 for the regression model between the total length and logarithm of Rohu's weight [10]. Similarly, high coefficients of determination were obtained between the weight and exponential fork length of Jackfish and Pickerel [11]. Therefore, the volume and weight of large fish fillets with a high degree of homogeneity may significantly correlate, suggesting the potential for determining the weight of a fish fillet from its volume for portioning purposes.

Smart cutting and robotics advances have long been introduced to the meat industry [12], [13]. Chickens could be cut into bun-sized portions, nuggets, or tapered-strip fillets of specified length and weight according to a template designed in a computer vision system (CVS) [14]. The weight of a chicken breast could be obtained by 3D scanning for economically optimized carcass cutting [15]. These advanced technologies also fostered automation in the fish industry. By applying X-ray technology, bones in a salmon fillet could be detected, and the fillet volume could be estimated for customized cutting and automated fillet packaging [16]–[18]. However, such X-ray solutions and corresponding systems are still costly and suitable only for large fish processing companies.

Machine vision has seen increasing growth in food evaluation and quality control in recent decades. As a non-destructive method, CVSs can be implemented for low-cost online applications in large-scale fish processing [19]. Many vision-based applications have been proposed for various fish processing tasks, such as post-trimming [20], blood defect detection [21], freezer burn identification [22], fish fillet authentication [23], and bone residue detection [24]. Based on CVSs, artificial intelligence was also applied to provide robust quality control of fish products. For example, deep learning could help to detect salmon muscle gaping for fillet grading [25]. Low-cost convolutional neural network models YOLOv5 and YOLOv8 were implemented in real time to detect salmon residues [26]. Laser projectors commonly coupled with machine vision were applied in 3D model reconstruction [27]–[29] and surface profiling [30]–[32]. However, few vision-based techniques for volume measurement from cross-sections have been developed for the meat industry [15]. Applying commercially available volume measurement and partitioning technologies will likely incur high implementation costs. Thus, developing low-cost CVSs for determining the fish fillet volume has considerable application potential. In addition, it is possible to extend a CVS with more advanced quality evaluation features, a few of which have been aforementioned.

As an initial effort towards developing low-cost technologies for fish processing, this study investigated a computer vision approach for determining fish fillet volume for optimal partitioning. The hardware was chosen for cost-efficiency and the potential development of stand-alone embedded systems for practical applications [33], [34]. Successfully developing such CVSs will show an outlook on cost-effective solutions for automated fillet portioning with advanced quality evaluation features, hence promoting customers' purchases of quality-controlled fish fillets with favorable weights, sizes, and shapes.

## 2. METHOD

### 2.1. Rationality of determining a fish fillet's weight from its volume

Portioning fish fillets into favorable slices based on their volumes for optimal packaging was proposed with the hypothesis of a linear relationship between a fillet's weight and volume. This relationship was validated in a preliminary study of catfish fillets obtained from local marts. As shown in Figure 1, a strong correlation between the weight and volume of catfish fillets was observed, with a significant coefficient of determination (*i.e.*,  $R^2=0.9432$ ). Therefore, a CVS was proposed to determine the fish fillet volume to support portioning high-value fish fillets with optimal weight to encourage a purchase decision. This CVS would also facilitate weight evaluation of portioned fillets when customers' affordability of high-value fillets or recommended daily serving amount is of concern.

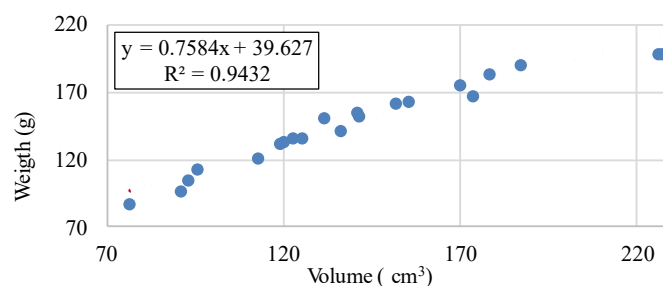


Figure 1. Relationship between the weight and volume of catfish fillets

## 2.2. System overview

Figure 2 shows an overview of the CVS developed to determine the fish fillet volume. The main components of this system include the following: i) A webcam (ACOME AWC11AWC, full HD, 30 fps) mounted on the ceiling of the image capture booth with a tilt angle of  $45^\circ$  was used; ii) A red line laser (SYD1230, 5 mW, wavelength of 650 nm) was used to determine the area of a cross-section of the sample; iii) A belt conveyor with dimensions of mm, which is driven by a stepper motor (Nema 17); iv) An image capture booth mounted on the belt conveyor; v) An STM32F103C8T6 Blue Pill development kit was used to control the belt conveyor system and receive control commands from a computer; and vi) A computer with a GUI was used for system control, image acquisition, and measurement of the fish fillet volume.

The working principle of the system is summarized as follows: i) When the sample is transported to the starting position for image acquisition, where the laser light is projected on the sample, the sample images are continuously acquired until the sample is out of the projected laser light; ii) The projected laser curve is detected from the images; iii) The area of the cross-section at the projected laser light is calculated; and iv) The sample volume is computed from the cross-sectional areas.

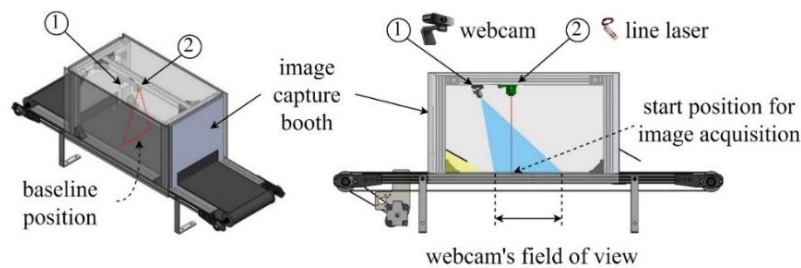


Figure 2. Overview of the proposed computer vision system

## 2.3. Algorithms for determining the volume of fish fillets

Let  $V$  be the volume of a sample transported on the belt conveyor with a constant speed  $v$ , passing by the projected laser light within a period  $\Delta t$  in which  $n$  images are captured. Let  $S_i$  be the volume of the cross-section area calculated from the  $i^{\text{th}}$  image. Although cross-section areas could be measured using stereo vision techniques [34], the single-camera approach was implemented for cost-effectiveness with acceptable accuracy. Figure 3 illustrates the concept of calculating the sample volume using a single camera from consecutive cross-section areas in Figure 3(a) and the distance between successive cross-sections in Figure 3(b).

$$V = \sum_{i=1}^n S_i \times d_i \quad (1)$$

where  $d_i$  is the travel distance of the sample between two consecutive image captures in Figure 3(b). Because the sample is transported at a constant speed, this so-called cross-section distance can be defined as (2).

$$d = d_i, i = [1, n] \quad (2)$$

Therefore, the sample volume can be computed as (3).

$$V = d \sum_{i=1}^n S_i = (v \times \Delta t) \sum_{i=1}^n S_i \quad (3)$$

The cross-section area of the  $i^{\text{th}}$  sample is calculated following the discrete integration principle, as illustrated in Figure 4.

$$S_i = \sum_j w_j h_j \quad (4)$$

where  $w_j$  and  $h_j$  are the width and height of a sampling point  $j$  on the sample surface at the cross-section in Figure 4(a), respectively. Thus, the area of a cross-section at the projected laser light can be computed from the location of the laser curve in the image as (5).

$$S_i = \sum_j (\text{width of } p_j) \times (\text{height of } p_j) \quad (5)$$

where pixel  $p_j$  on the detected laser curve in Figure 4(b) corresponds to the sampling point  $j$  on the sample surface. It should be noted that  $h_j$  corresponds to the pixel distance  $(y_j - y_b)$  from  $p_j$  to the baseline at the start position for image acquisition, as depicted in Figure 2.

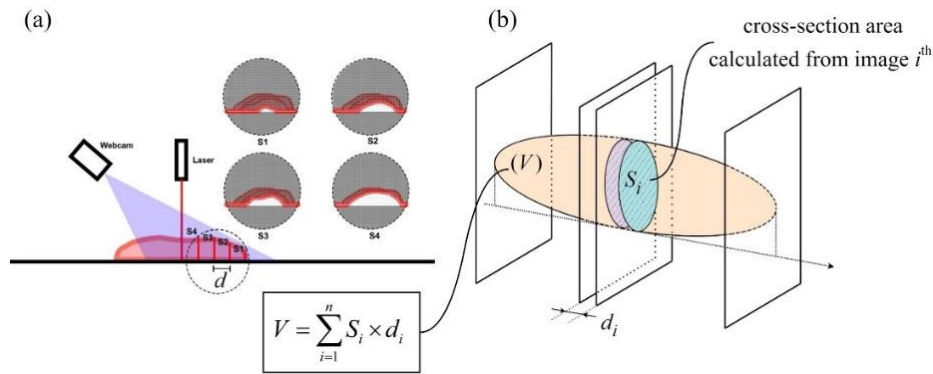


Figure 3. Illustration of (a) the volume calculation principle from (b) cross-section areas

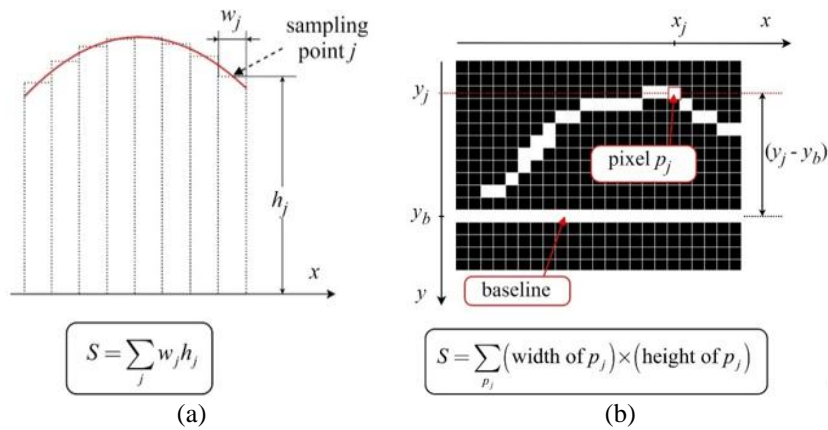


Figure 4. Calculating a cross-section area (a) illustrated in the 2D coordinates and (b) applied in an image of the projected laser light on the sample

**2.3.1. Detection of the projected laser curve on the fillet**

Figure 5 shows the main steps for detecting the laser curve critical for calculating cross-section areas of the sample. From the original image in Figure 5(a), a region of interest is selected in Figure 5(b) to reduce unnecessary computations [35]. Then, Gaussian blur is applied to the cropped image with kernel size  $(5 \times 5)$  to remove noise [36], followed by thresholding in the HSV color space with low and high thresholds of  $[154, 0, 155]$  and  $[180, 0, 155]$ , respectively. An example of an image after being filtered and thresholded is depicted in Figure 5(c), showing the laser curve of bright pixels whose intensity values were 255. For an accurate cross-section area calculation, thinning was performed. Considering each column of the image matrix, the intensity of all bright pixels except the middle pixel was converted to 0. As a result, the laser curve was thinned, consisting of single pixels on consecutive columns of the image matrix in Figure 5(d). An illustration of this thinning algorithm is presented in Figure 6.

**2.3.2. Calculation of the cross-section area based on the projected laser curve**

The sample was captured from the webcam with a tilt angle of  $45^\circ$ ; therefore, the actual width of a pixel  $p_j$  and its distance from the baseline  $(y_j - y_b)$  depended on its vertical coordinate  $y_j$ . As shown in Figure 7, camera calibration was implemented to correct any distortion [34], and the corners on the chessboard were detected. With the known dimensions of the squares on the chessboard, a function was obtained to calculate the pixel width from its vertical coordinate. Another function was fitted based on the actual height of the corners of the belt conveyor and its distance from the baseline.

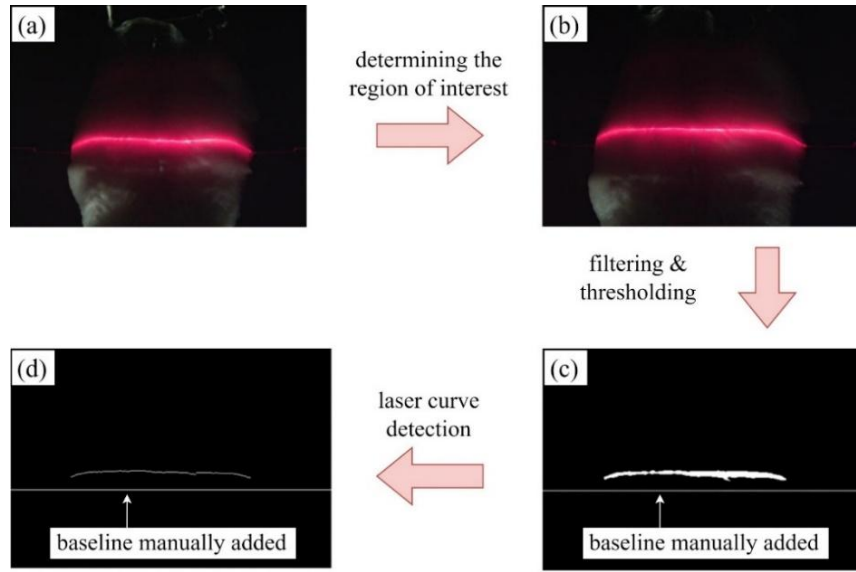


Figure 5. Illustration of the main steps for detecting the laser curve projected on the sample surface: (a) an original image of the projected laser light, (b) region of interest determination, (c) filtering and thresholding the region of interest, and (d) thinning the thresholded image

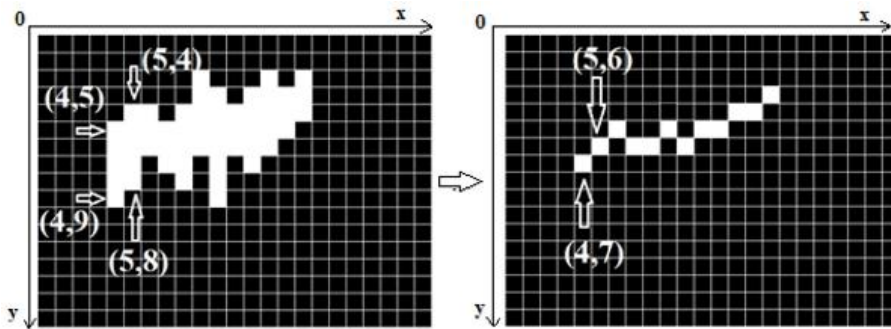


Figure 6. Thinning of a detected laser curve

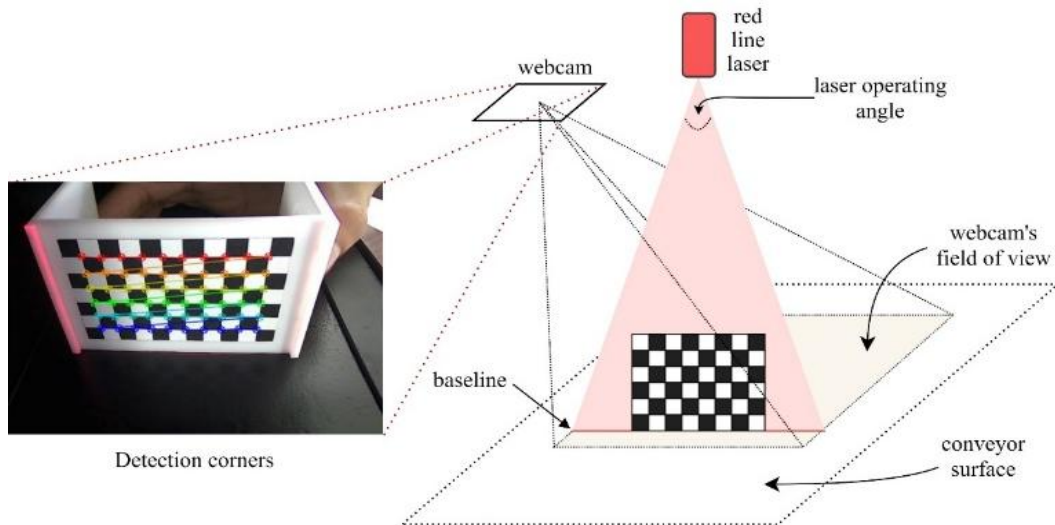


Figure 7. Camera calibration setup



## 2.4. Assessment of system performance

The measurement error  $e$  and percent error  $\delta$  were calculated to assess the system performance.

$$e = V_m - V_a \quad (6)$$

$$\delta = \frac{|V_m - V_a|}{V_a} \times 100\% \quad (7)$$

where  $V_m$  and  $V_a$  are the measured and actual volumes of a sample, respectively.

## 3. RESULTS AND DISCUSSION

### 3.1. Effect of the conveyor speed

With a fixed frame rate of the webcam, the conveyor speed was an essential factor in calculating the sample volume because it determined the cross-section distance  $d$ , which was the distance between two consecutive cross-sections whose areas could be calculated in Figure 2. Figure 8 shows two kinds of objects under investigation. As shown in Figure 8(a), a cuboid wood sample of approximately 3.5 x 4.0 x 4.0 cm<sup>3</sup> was used to investigate the effect of the conveyor speed so that the optimal conveyor speed will be implemented to calculate the system performance with catfish fillets in Figure 8(b).

Table 1 shows the performance of the system with varying conveyor speeds. Operating the system at a conveyor speed of 30.6 mm/s resulted in a measurement percent error of approximately 5.0%. A lower operation speed of 7.5 mm/s led to a slightly larger percent error of approximately 6.1% (approximately 0.6-cm<sup>3</sup> mean error); however, it would be more precise considering a smaller standard deviation. Although the system could achieve higher throughput with a greater translational speed of the conveyor, it might result in less accuracy when evaluated with a sample with a rough surface as a trade-off. Therefore, a conveyor speed of 7.5 mm/s was chosen for higher precision and accuracy for samples with irregular surfaces.

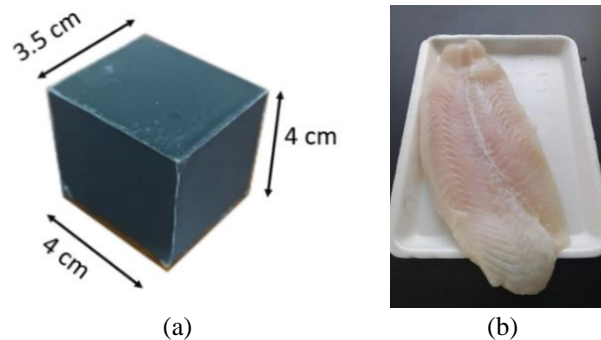


Figure 8. Sample types for evaluating the system accuracy: (a) a wood cuboid and (b) a catfish fillet

Table 1. Measurement of a cubic wood sample at different conveyor speeds

Speed (mm/s)	Mean $\pm$ standard deviation (cm <sup>3</sup> )	Percent error (%)
7.5	52.5 $\pm$ 0.8	6.1
15.3	53.5 $\pm$ 1.0	4.3
30.6	53.1 $\pm$ 1.4	5.0
61.2	38.7 $\pm$ 4.0	30.8

### 3.2. Evaluation of system accuracy

#### 3.2.1. Evaluation with artificial samples of different volumes

Table 2 shows the system's accuracy initially evaluated with wood cuboids of different volumes. The greatest percent error was 15.7%, corresponding to the error of 4.7 cm<sup>3</sup> observed with a 30 cm<sup>3</sup> cuboid. The smallest percent error was only 2.9%, corresponding to the absolute error of 4.3 cm<sup>3</sup> observed with a 150-cm<sup>3</sup> cuboid. With comparable absolute errors, these results demonstrated that the percent errors were larger for smaller samples, which can be explained by the formula for calculating the percent error significantly depending on the sample volume in (7). The mean absolute error was only about 4.2 cm<sup>3</sup>, indicating a potential for measuring the area of large fish fillets for automated and customized partitioning.

Table 2. Measurement of cubic wood samples with different volumes

Actual volume (cm <sup>3</sup> )	Measured volume (cm <sup>3</sup> )	Error (cm <sup>3</sup> )	Percent error (%)
30.0	34.7	4.7	15.7
30.3	31.3	1.0	3.3
55.9	62.8	6.9	12.3
56.2	61.8	5.6	10.0
60.0	63.4	3.4	5.7
62.9	66.5	3.6	5.7
150.0	145.7	-4.3	2.9

### 3.2.2. Evaluation with catfish fillets

The system performance was also evaluated with catfish fillets purchased from local marts. Table 3 shows the measurement statistics with samples ranging from 142.2 to 225.4 cm<sup>3</sup> in area. The errors were in the range of [8.5; 28.9] cm<sup>3</sup>. According to the regression between the volume and weight of catfish fillets in Figure 1, the maximum error of 28.9 cm<sup>3</sup> corresponds to a weight estimation error of about 22 g in a portioned fillet, which will not likely affect a customer's purchase intention.

The percent error was within [3.8%; 17.0%], with a mean of approximately 9.2%. The measured volumes were greater than the actual volumes, which could be due to the rough surfaces of the samples leading to a slightly inaccurate estimation of the volume between two consecutive cross-sections. These errors can be minimized with an increased capture frame rate to reduce the cross-section distance for more accurate volume measurement by the discrete integration principle. Table 3 shows less significant measurement errors for larger samples. Because the samples were portioned fillets purchased from local marts, the system will be more accurate in measuring fillet volumes when applied in the automated portioning of large fish fillets.

Table 3. Measurement of catfish fillets with different volumes

Actual volume (cm <sup>3</sup> )	Measured volume (cm <sup>3</sup> )	Error (cm <sup>3</sup> )	Percent error (%)
142.2	156.7	14.5	10.2
151.6	166.6	15.0	9.9
170.5	199.4	28.9	17.0
179.1	199.3	20.2	11.3
187.0	201.8	14.8	7.9
225.0	235.4	10.4	4.6
225.4	233.9	8.5	3.8

## 4. CONCLUSION

In this study, a low-cost CVS was introduced to measure the volume of fish fillets. The system could be operated at conveyor translational speeds ranging from 7.5 to 30.6 mm/s. The system had a mean absolute percent error of about 9.2% when measuring catfish fillets with rough surfaces. It was more accurate with larger samples, indicating its efficient use for volume measurement of large fish fillets. With a strong relationship between the volume and weight of a fish fillet, the proposed CVS can be used to determine the weight of large fish fillets for subsequent partitioning into portions with favorable sizes, weights, and shape patterns for optimal packaging. Because a CVS can be extended with more vision-based features, advanced quality control features such as shape uniformity and defect detection can be integrated into the system. Therefore, the proposed CVS shows considerable potential for developing a cost-effective automated system for partitioning and quality classification of high-valued fish fillets.

## REFERENCES




- [1] J. Chen, M. Jayachandran, W. Bai, and B. Xu, "A critical review on the health benefits of fish consumption and its bioactive constituents," *Food Chemistry*, vol. 369, Feb. 2022, doi: 10.1016/j.foodchem.2021.130874.
- [2] P. Xun *et al.*, "Fish consumption and risk of stroke and its subtypes: accumulative evidence from a meta-analysis of prospective cohort studies," *European Journal of Clinical Nutrition*, vol. 66, no. 11, pp. 1199–1207, Oct. 2012, doi: 10.1038/ejcn.2012.133.
- [3] J. Zheng, T. Huang, Y. Yu, X. Hu, B. Yang, and D. Li, "Fish consumption and CHD mortality: an updated meta-analysis of seventeen cohort studies," *Public Health Nutrition*, vol. 15, no. 4, pp. 725–737, Sep. 2012, doi: 10.1017/S1368980011002254.
- [4] A. Lofstedt, B. de Roos, and P. G. Fernandes, "Less than half of the European dietary recommendations for fish consumption are satisfied by national seafood supplies," *European Journal of Nutrition*, vol. 60, no. 8, pp. 4219–4228, May 2021, doi: 10.1007/s00394-021-02580-6.
- [5] R. H. Thurstan and C. M. Roberts, "The past and future of fish consumption: Can supplies meet healthy eating

- recommendations?," *Marine Pollution Bulletin*, vol. 89, no. 1–2, pp. 5–11, Dec. 2014, doi: 10.1016/j.marpolbul.2014.09.016.
- [6] H. S. Solgaard, Y. Yang, and T. T. Nguyen, "An investigation of consumers' preference and willingness to pay for fish welfare in Denmark: A discrete choice modeling approach," *Aquaculture*, vol. 574, Sep. 2023, doi: 10.1016/j.aquaculture.2023.739652.
- [7] D. Menozzi *et al.*, "Consumers' preferences and willingness to pay for fish products with health and environmental labels: Evidence from five European countries," *Nutrients*, vol. 12, no. 9, pp. 1–22, Aug. 2020, doi: 10.3390/nu12092650.
- [8] J. Cantillo, J. C. Martín, and C. Román, "Discrete choice experiments in the analysis of consumers' preferences for finfish products: A systematic literature review," *Food Quality and Preference*, vol. 84, Sep. 2020, doi: 10.1016/j.foodqual.2020.103952.
- [9] N. T. Thong, Q. T. K. Ngoc, and G. Voldnes, "Consumer's perception and acceptance of lumpfish used in salmon cages," *Aquaculture International*, vol. 32, no. 3, pp. 2331–2352, Oct. 2024, doi: 10.1007/s10499-023-01273-7.
- [10] P. Jayraj, R. Machavaram, G. Sahu, and V. Paradkar, "Measurement of morphometric dimensions and mechanical properties of Rohu fish for design of processing machines," *Journal of Aquatic Food Product Technology*, vol. 28, no. 2, pp. 150–164, Feb. 2019, doi: 10.1080/10498850.2019.1569741.
- [11] C. McAuley, D. Smith, A. Dersch, B. Koppe, S. Mouille-Malbeuf, and D. Sowan, "Whole fish vs. fish fillet—The risk implications for First Nation subsistence consumers," *Cogent Food and Agriculture*, vol. 4, no. 1, Jan. 2018, doi: 10.1080/23311932.2018.1546790.
- [12] A. Mason, D. Romanov, L. E. Cordova-Lopez, S. Ross, and O. Korostynska, "Smart knife: technological advances towards smart cutting tools in meat industry automation," *Sensor Review*, vol. 42, no. 1, pp. 155–163, Jan. 2022, doi: 10.1108/SR-09-2021-0315.
- [13] W. Xu *et al.*, "Robotization and intelligent digital systems in the meat cutting industry: from the perspectives of robotic cutting, perception, and digital development," *Trends in Food Science and Technology*, vol. 135, pp. 234–251, May 2023, doi: 10.1016/j.tifs.2023.03.018.
- [14] B. Heck, "Automated chicken processing machine vision and water-jet cutting for optimized performance," *IEEE Control Systems*, vol. 26, no. 3, pp. 17–19, Jun. 2006, doi: 10.1109/MCS.2006.1636305.
- [15] L. Adamczak, M. Chmiel, T. Florowski, D. Pietrzak, M. Witkowski, and T. Barczak, "The use of 3D scanning to determine the weight of the chicken breast," *Computers and Electronics in Agriculture*, vol. 155, pp. 394–399, Dec. 2018, doi: 10.1016/j.compag.2018.10.039.
- [16] D. Mery *et al.*, "Automated fish bone detection using X-ray imaging," *Journal of Food Engineering*, vol. 105, no. 3, pp. 485–492, Aug. 2011, doi: 10.1016/j.jfoodeng.2011.03.007.
- [17] Marel, "Flexicut pinbone removal and portioning," *marel.com*, <https://marel.com/en/products/flexicut/> (accessed Feb. 25, 2024).
- [18] H. Einarssdóttir, B. Guðmundsson, and V. Ómarsson, "Automation in the fish industry," *Animal Frontiers*, vol. 12, no. 2, pp. 32–39, Apr. 2022, doi: 10.1093/af/vfac020.
- [19] M. N. Madhubhashini, C. P. Liyanage, A. U. Alahakoon, and R. P. Liyanage, "Current applications and future trends of artificial senses in fish freshness determination: A review," *Journal of Food Science*, vol. 89, no. 1, pp. 33–50, Dec. 2024, doi: 10.1111/1750-3841.16865.
- [20] E. Bar *et al.*, "Towards robotic post-trimming of salmon fillets," *Industrial Robot*, vol. 43, no. 4, pp. 421–428, Jun. 2016, doi: 10.1108/IR-11-2015-0205.
- [21] E. Misimi, E. R. Øye, Ø. Sture, and J. R. Mathiasen, "Robust classification approach for segmentation of blood defects in cod fillets based on deep convolutional neural networks and support vector machines and calculation of gripper vectors for robotic processing," *Computers and Electronics in Agriculture*, vol. 139, pp. 138–152, Jun. 2017, doi: 10.1016/j.compag.2017.05.021.
- [22] J. L. Xu and D. W. Sun, "Identification of freezer burn on frozen salmon surface using hyperspectral imaging and computer vision combined with machine learning algorithm," *International Journal of Refrigeration*, vol. 74, pp. 149–162, Feb. 2017, doi: 10.1016/j.ijrefrig.2016.10.014.
- [23] S. Grassi, E. Casiraghi, and C. Alamprese, "Fish fillet authentication by image analysis," *Journal of Food Engineering*, vol. 234, pp. 16–23, Oct. 2018, doi: 10.1016/j.jfoodeng.2018.04.012.
- [24] T. Xie, X. Li, X. Zhang, J. Hu, and Y. Fang, "Detection of Atlantic salmon residues based on computer vision," *Food Control*, vol. 123, May 2021, doi: 10.1016/j.foodcont.2020.107787.
- [25] J. L. Xu and D. W. Sun, "Computer vision detection of salmon muscle gaping using convolutional neural network features," *Food Analytical Methods*, vol. 11, no. 1, pp. 34–47, Jan. 2018, doi: 10.1007/s12161-017-0957-4.
- [26] Y. Feng, X. Li, Y. Zhang, and T. Xie, "Detection of Atlantic salmon residues based on computer vision," *Journal of Food Engineering*, vol. 358, Dec. 2023, doi: 10.1016/j.jfoodeng.2023.111658.
- [27] H. C. Nguyen and B. R. Lee, "3D model reconstruction system development based on laser-vision technology," *International Journal of Automation Technology*, vol. 10, no. 5, pp. 813–820, Sep. 2016, doi: 10.20965/ijat.2016.p0813.
- [28] X. Wang, Z. Zhu, F. Zhou, and F. Zhang, "Complete calibration of a structured light stripe vision sensor through a single cylindrical target," *Optics and Lasers in Engineering*, vol. 131, Aug. 2020, doi: 10.1016/j.optlaseng.2020.106096.
- [29] T. Yang, S. Wu, S. Zhang, S. Yang, Y. Wu, and F. Liu, "A robust and accurate centerline extraction method of multiple laser stripe for complex 3D measurement," *Advanced Engineering Informatics*, vol. 58, Oct. 2023, doi: 10.1016/j.aei.2023.102207.
- [30] B. A. Abu-Nabah, A. O. ElSoussi, and A. E. R. K. Al Alami, "Simple laser vision sensor calibration for surface profiling applications," *Optics and Lasers in Engineering*, vol. 84, pp. 51–61, Sep. 2016, doi: 10.1016/j.optlaseng.2016.03.024.
- [31] Y. Wang, B. Yu, X. Zhang, and J. Liang, "Automatic extraction and evaluation of pavement three-dimensional surface texture using laser scanning technology," *Automation in Construction*, vol. 141, Sep. 2022, doi: 10.1016/j.autcon.2022.104410.
- [32] K. He, C. Sui, T. Huang, R. Dai, C. Lyu, and Y. H. Liu, "3D surface reconstruction of transparent objects using laser scanning with LTFTF method," *Optics and Lasers in Engineering*, vol. 148, Jan. 2022, doi: 10.1016/j.optlaseng.2021.106774.
- [33] A. I. M. Anuar, R. Mohamad, A. M. Markom, and R. Concepcion, "Real-time forest fire detection, monitoring, and alert system using Arduino," *Indonesian Journal of Electrical Engineering and Computer Science*, vol. 33, no. 2, pp. 942–950, Feb. 2024, doi: 10.11591/ijeecs.v33.i2.pp942-950.
- [34] N. M. Hussien, Y. M. Mohialden, N. T. Ahmed, M. A. Mohammed, and T. Sutikno, "A smart gas leakage monitoring system for use in hospitals," *Indonesian Journal of Electrical Engineering and Computer Science*, vol. 19, no. 2, pp. 1048–1054, Aug. 2020, doi: 10.11591/ijeecs.v19.i2.pp1048-1054.
- [35] C. N. Nguyen, V. L. Lam, P. H. Le, H. T. Ho, and C. N. Nguyen, "Early detection of slight bruises in apples by cost-efficient near-infrared imaging," *International Journal of Electrical and Computer Engineering*, vol. 12, no. 1, pp. 349–357, Feb. 2022, doi: 10.11591/ijece.v12i1.pp349-357.
- [36] M. P. Pavan Kumar, B. Poornima, H. S. Nagendraswamy, C. Manjunath, and B. E. Rangaswamy, "A refined structure preserving image abstraction framework as a pre-processing technique for desire focusing on prominent structure and artistic stylization," *Vietnam Journal of Computer Science*, vol. 8, no. 4, pp. 529–583, May 2021, doi: 10.1142/S2196888822500038.






## BIOGRAPHIES OF AUTHORS






**Chanh-Nghiem Nguyen**    received a master's degree in mechatronics from Asian Institute of Technology, Pathumthani, Thailand, in 2007 and a Ph.D. degree from Graduate School of Engineering Science, Osaka University, Osaka, Japan, in 2012. Since 2005, he has worked at the Faculty of Automation Engineering, College of Engineering Technology, Can Tho University. He is currently an associate professor at Faculty of Automation Engineering and is in charge of Automation Laboratory. His research interests include computer vision, postharvest technologies, control systems, GNSS applications, machine learning, and multispectral/hyperspectral imaging and applications. He can be contacted at email: ncngkiem@ctu.edu.vn.






**Ngoc-Tan Vo**    graduated in mechatronics from Faculty of Automation Engineering, College of Engineering, Can Tho University, Vietnam, in 2021. His research interests include mechatronics, embedded systems, image processing, robotics, and computer vision. He can be contacted at email: tanafgh@gmail.com.






**Ngoc-Thanh Nguyen**    graduated in mechatronics from Faculty of Automation Engineering, College of Engineering, Can Tho University, Vietnam in 2021. His research interests include mechatronics, embedded systems, image processing, robotics, and computer vision. He can be contacted at email: thanhng020301@gmail.com.



**Nhut-Thanh Tran**    received a bachelor's degree in mechatronics from Can Tho University, Vietnam, in 2008 and an M.Eng. degree in automation from Ho Chi Minh City University of Technology, Vietnam, in 2011. He is a senior lecturer at Faculty of Automation Engineering, Can Tho University, Vietnam, since 2012. The degree of Ph.D. in engineering design was awarded by Kyoto Institute of Technology, Japan, in 2021. His research interests include automated systems, precision agriculture, spectroscopy applications, and image analysis. He can be contacted at nhutthanh@ctu.edu.vn.



**Chi-Ngon Nguyen**    received his bachelor's and master's degrees in electronic engineering from Can Tho University and the Vietnam National University, Ho Chi Minh City University of Technology, in 1996 and 2001, respectively. The Ph.D. degree was awarded by the University of Rostock, Germany, in 2007. Since 1996, he has worked at the Can Tho University. Currently, he is an associate professor in automation at Faculty of Automation Engineering and a Vice Chairman of the Board of Trustees of Can Tho University. He is also a nationally distinguished lecturer and a secretary of the National Council for Professorships in electrical-electronics and automation. His research interests are AI applications, intelligent control, medical control, pattern recognition, classifications, computer vision, and agricultural automation. He can be contacted at email: ncngon@ctu.edu.vn.